

<https://doi.org/10.1038/s41698-024-00795-4>

Comprehensive analysis of targetable mutations and tumor microenvironment in urachal cancer



David J. Benjamin¹ ✉, Tolulope T. Adeyelu², Andrew Elliott², Sourat Darabi¹, Thomas Lee³, Rana R. McKay⁴, Matthew J. Oberley² & Arash Rezazadeh Kalebasty⁵

Urachal cancer, a rare malignancy, generally presents in the clinical setting with advanced stages of disease. Systemic treatment with chemotherapy is generally utilized in this setting. However, there remains a paucity of data on the effectiveness of immune checkpoint inhibitors or targeted therapies for urachal cancer. We analyzed the genomic profile of urachal cancer in order to identify potentially targetable mutations and evaluate the tumor microenvironment. 42 urachal samples were retrospectively analyzed. Our results showed that TP53, GNAS and KRAS mutations were common in urachal cancer with increased prevalence of *TP53* mutation in urachal cohorts without MAPK-alterations. The tumor microenvironment demonstrated increased NK cells in MAPK-altered urachal cancer. Finally, we show that urachal cancer shares genomic and transcriptomic similarity with colorectal cancer compared to bladder cancer. This study provides new insights into the molecular profiles of urachal tumor samples and possibility of association with colorectal cancer that might guide future clinical trial design.

Urachal cancer is a rare genitourinary malignancy that accounts for less than 1% of bladder cancers¹. Urachal cancer originates from the remnant that connects the fetal bladder and allantois². Although the urachus generally obliterates at birth, it may persist in approximately one-third of individuals and in some cases, lead to malignancy. Individuals with urachal cancer generally present with advanced stages of disease, with symptoms such as hematuria, abdominal pain, fatigue and weight loss. Given that adenocarcinoma is the most common histology in up to 80% of instances, additional work-up such as colonoscopy is generally performed to evaluate for a colorectal origin of malignancy³.

Population-level studies have shown that men in the fifth decade of life account for the majority of cases of this uncommon cancer. Data from the California Cancer Registry consisting of 315 cases of urachal cancer found no differences in survival based on demographic factors, such as sex, ethnicity or neighborhood socioeconomic status⁴. Given the rarity of this malignancy, retrospective data to date has not readily identified risk factors leading to the development of urachal cancer.

While en bloc surgical resection is the preferred treatment approach for localized disease, systemic treatment with chemotherapy is employed for recurrent or advanced stages of urachal cancer⁵. Due to a lack of prospective data, treatment approaches for advanced urachal cancer are based on case

series and small prospective cohort studies, including non-transitional cell carcinoma subtypes involving 5-fluorouracil (5-FU) and cisplatin^{2,6,7}. A meta-analysis of 1010 cases of urachal cancer identified that combination therapies including both cisplatin and 5-fluorouracil achieved improved survival compared to regimens consisting of only one of the two agents⁸. There are only two known reported uses of immune checkpoint inhibitors in treating advanced urachal cancer, and one report of targeted therapy tepotinib, a mesenchymal-epithelial transition (cMET) inhibitor, being used in treating urachal cancer^{9–11}.

Several studies have examined the genomic landscape of urachal cancers to better understand the malignancy and identify potentially actionable mutations. The largest study of urachal cancer involving 70 tumors identified mutations in the following genes: *TP53* (66%), *KRAS* (21%), *BRAF* (4%), *PIK3CA* (4%), *MET* (1%) and *NRAS* (1%)¹². Additionally, ten tumors were found to have PD-L1 expression including one with a tumor proportion score (TPS) of greater than or equal to 50% and nine samples exhibiting TPS of 1–49%. A separate single-center study of 30 tumor specimens revealed that the most common mutations were *TP53* (83%), *KRAS* (30%) and *GNAS* (27%). Finally, a study by Kardos and colleagues evaluating 12 urachal cancer specimens demonstrated similar mutations in *TP53* (100%), *MTOR* (33%), *APC* (25%) and *NF1* (25%)⁹. In

¹Hoag Family Cancer Institute, Newport Beach, CA, 92663, USA. ²Caris Life Sciences, Irving, TX, 75039, USA. ³Hoag Memorial Hospital Presbyterian, Newport Beach, CA, 92663, USA. ⁴University of California, San Diego Health, La Jolla, CA, USA. ⁵University of California, Irvine, Orange, CA, 92868, USA. ✉e-mail: David.Benjamin@hoag.org

addition, transcriptional analysis of the tumors was compared to tissues of origin in The Cancer Gene Atlas (TCGA), revealing that five urachal tumors closely resembled colon and rectal (COADREAD) tumors and four were similar to glioblastoma (GBM) tumors. Despite these aforementioned studies, there remains a paucity of data on the molecular profile of urachal cancer relative to more common genitourinary malignancies such as prostate and bladder cancer.

Given the growing role of next-generation sequencing in determining treatment choices in the clinical setting and in light of genomic alterations more commonly observed in colorectal cancer rather than bladder cancer, we performed a retrospective study molecularly profiling urachal cancer samples from a commercial database of patients treated at various cancer centers throughout the United States. We characterized the genomic landscape and tumor microenvironments of these urachal cancers and performed central pathology review to further examine associations with histological features that provide new insights to the biology of this rare disease.

Results

Patient cohorts

Forty-two (42) urachal cases (UrC) were included in this study, with median age of 58.5 years (range: 24–86) and of which 54.8% ($n = 23$) were female. Histological review revealed that samples were comprised of 40% ($n = 17$) mucinous adenocarcinoma and 24% ($n = 10$) enteric adenocarcinoma, while 36% ($n = 15$) had mixed histologies. Urachal patients were then subdivided into MAPK-Altered ($n = 22$), and MAPK-WT ($n = 20$) based on the presence of MAPK-associated gene alterations. The demographics of these samples are shown in Table 1.

Genomic landscape of urachal cancer

Globally, alterations in urachal cancer included mutation in *TP53* ($n = 37$, 83.3%), *KRAS* ($n = 18$, 42.86%), *GNAS* ($n = 5$, 11.9%), *SMAD4* ($n = 4$, 9.5%), *PIK3CA* ($n = 4$, 9.5%) – Fig. 1a. *KRAS* mutation codon changes includes G12V ($n = 5$), G12D ($n = 5$), G13D ($n = 3$), G12S ($n = 1$) and Q61H ($n = 1$). The prevalence of *TP53* mutation was significantly higher in MAPK-Altered vs MAPK-WT tumors (100% vs 68.5%, $p = 0.0092$). The prevalence of *GNAS* (18.2% vs 5.0%, $p = 0.346$) and *PIK3CA* (13.6% vs 5.0%, $p = 0.598$) had numerical increase in MAPK-Altered while *SMAD4* (4.5% vs 15%, $p = 0.433$) showed numerical increase in MAPK-WT UrC – Fig. 1b. No alteration in dMMR/MSI-H was observed across all urachal samples analyzed.

Immune landscape of urachal cancer

The immune landscape of urachal cancer (UrC) included low programmed death-ligand 1 [PD-L1] expression across the samples: 11.76% ($n = 4$) had CPS score ≥ 10 , 55.88% ($n = 19$) had CPS score of 1–9, while 32.35% ($n = 11$) had a combined positive score (CPS) score of 0 – Fig. 1c. Furthermore, predictive markers of response to immunotherapy – tumor mutation burden-high [TMB-H] (4.78% vs 4.87%, $p = 1.0$) and PD-L1 (11.76% vs 11.76%, $p = 1.0$) – were similar in both Mitogen activated protein kinase (MAPK)-Altered and MAPK-wild type (WT) UrC – Fig. 1d. Similarly, no difference in the distribution of interferon (IFN)-gamma scores (a transcriptomic signature predictive of response to immunotherapy) was observed between MAPK-Altered and MAPK-WT UrC (Median: -0.36 vs -0.38 , $p = 0.052$) – Fig. 1e. Using quanTIseq to deconvolve transcriptomic profiles and estimate immune cell fractions, the tumor microenvironment was similar across the MAPK-Altered and MAPK-WT cohorts, with exception of NK cells, which were significantly higher in MAPK-Altered UrC patients (3.5% vs 2.7%, $p = 0.022$) – Fig. 1f. Meanwhile, overall survival was similar between MAPK-Altered and -WT urachal cancer (HR: 1.05, 95% CI 0.48–2.31) and no prognostic impact of MAPK-alterations was observed in these patients (Supplementary Fig. 1a/b) – using surrogates of time from diagnosis and tissue collection to last contact. Outcome data shows that 7 urachal patients were treated with IO therapy (Atezolizumab, Avelumab, Ipilimumab, Nivolumab or Pembrolizumab) but no therapeutic

Table 1 | Demographics of analyzed tumor samples

Characteristic	Total	MAPK-Altered	MAPK-WT	p-value
Total, N (%)	42	22	20	
Age				
Median age [Range, years]	58.5 [24–86]	65 [24–86]	56.5 [31–83]	0.219
Sex				
Male, N (%)	19 (45.2%)	11 (50%)	8 (40%)	0.516
Female, N (%)	23 (54.8%)	11 (50%)	12 (60%)	
Histology				
Mucinous	17 (40%)	10 (45.5%)	7 (35%)	0.430
Enteric	10 (24%)	5 (22.7%)	5 (25%)	
Others ^a	15 (36%)	7 (31.8%)	8 (40%)	
Specimen sites				
Bladder/urachus	23 (54.8%)	10 (45.5%)	13 (65.0%)	0.574
Other sites ^b	19 (45.2%)	12 (54.5%)	7 (35%)	
Race				
White	17 (40.5%)	9 (40.9%)	8 (40.0%)	0.877
Black	4 (9.5%)	3 (13.6%)	1 (5.0%)	
Asian	6 (14.3%)	3 (13.6%)	3 (15.0%)	
Others	3 (7.1%)	0 (0.0%)	3 (15.0%)	
Not reported	12 (28.6%)	7 (31.8%)	5 (25.0%)	
Ethnicity				
Hispanic	9 (21.4%)	3 (13.6%)	6 (30.0%)	1.000
Non-Hispanic	23 (54.8%)	11 (50.0%)	12 (60.0%)	
Not reported	10 (23.8%)	8 (36.4%)	2 (10.0%)	

^aOthers histology include – Mixed, signet ring cell, adenocarcinoma, non-adeno with plasmacytoid features.

^bOthers include specimen sites such as lungs, pelvic wall, small bowels, fornix of vagina, brain, abdomen, skin and connective tissues.

advantage was observed in these patients as the median OS from therapy to last contact was 10 months (95% CI, 2–15 months).

We analyzed the genomic and transcriptomic differences among urachal histological subtypes—mucinous, enteric, and others. While no significant differences were observed in mutation prevalence across the three groups, we noted a non-significant trend toward higher prevalence of PD-L1 (22c3) expression and TMB-High in the enteric subtype compared to Fig. 2 mucinous and other subtypes. Analysis of the tumor microenvironment revealed a significant reduction in M2 macrophages and an increase in dendritic cells in enteric urachal cancers. However, no significant differences in overall survival (OS) were observed among these groups. (Supplementary Fig. 2)

Genomic profile of urachal cancer in comparison to bladder and colorectal

As the origin of urachal cancer remains an ongoing debate in the genitourinary cancer field, the genomic profile of urachal cancer ($n = 42$) was evaluated in comparison to colorectal ($n = 21,136$) and bladder cancer ($n = 6455$). The prevalence of *TP53* (83.3% vs 73.7%, 58.8%, $p = 0.0019$), *GNAS* (11.9% vs 2.8% vs 0.1%, $p < 0.0001$) and *STK11* (7.1% vs 0.4% vs 0.5%, $p = 0.002$) mutations was significantly higher in urachal cancer compared to bladder or CRC. Genomic loss-of-heterozygosity (gLOH) was significantly higher in UrC (29.0% vs 10.8%, $p = 0.0044$), while the prevalence of *APC* mutation (4.8% vs 75.0%, $p < 0.0001$) was significantly lower compared to CRC. Similarly, mutation of *SMAD4* (9.5% vs 1.1%, $p = 0.0014$) and *KRAS* (35.7% vs 3.6%, $p < 0.0001$) was significantly higher in UrC, while the prevalence of *RBI* (5.5% vs 19.9%, $p = 0.024$), *TERT* promoter (p*TERT*)

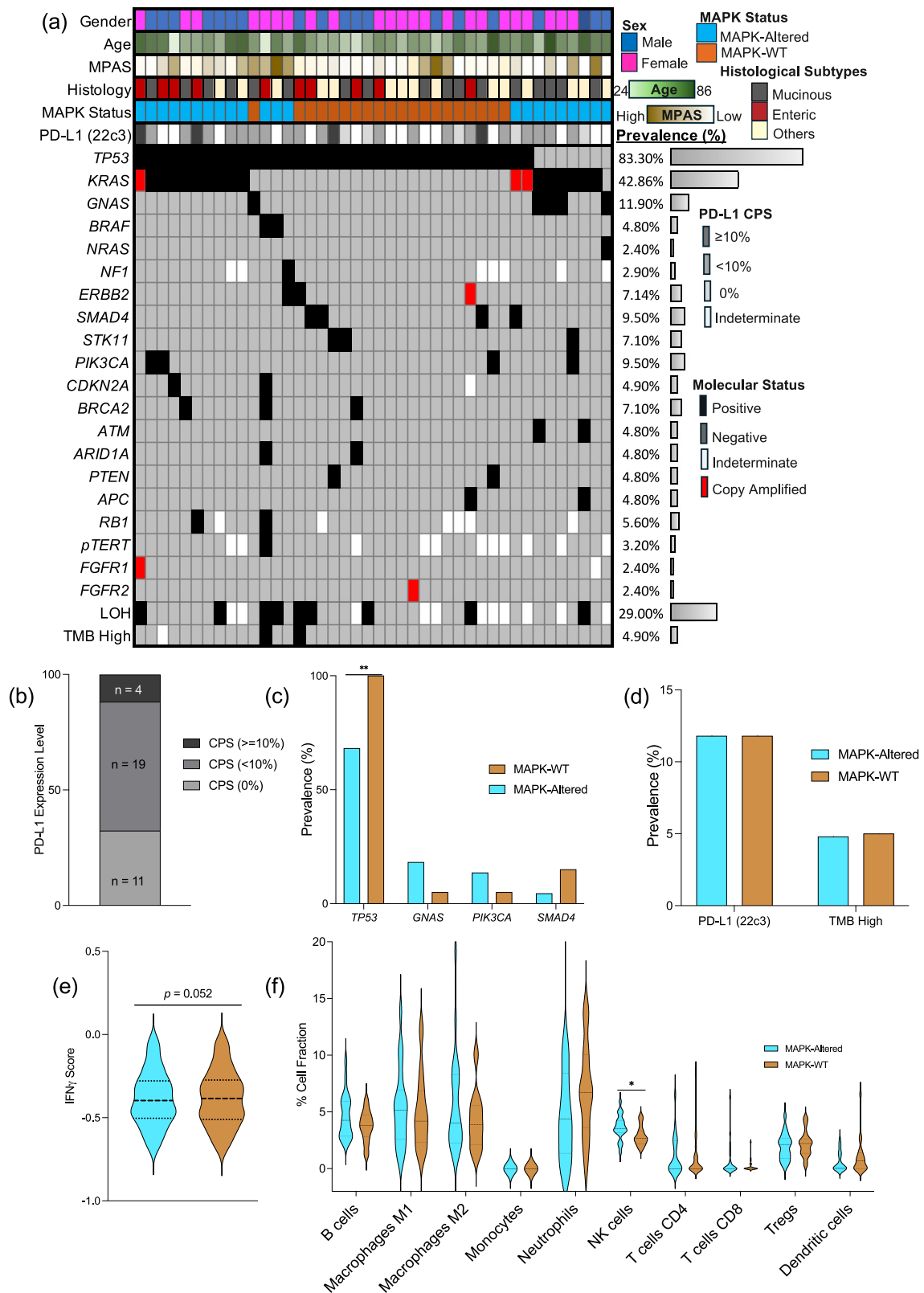


Fig. 1 | Genomic alterations in urachal cancer (UrC). **a** Oncoprint displaying the overall genomic landscape of pathogenic/likely pathogenic alterations in UrC. **b** Mutational changes in selected genes between Mitogen activated protein kinase (MAPK)-Altered and MAPK-wild type (WT). **c** Predictive markers of immunotherapy response between MAPK-Altered and MAPK-WT UrC. **d** Distribution of

programmed death-ligand 1 [PD-L1] expression by immunohistochemistry. **e** Interferon gamma signature compared between MAPK-altered and MAPK-WT urachal cancer. **f** Tumor microenvironment compared between MAPK-Altered and MAPK-WT UrC. Asterisks indicates statistical significance, * $p < 0.05$, ** $p < 0.01$.

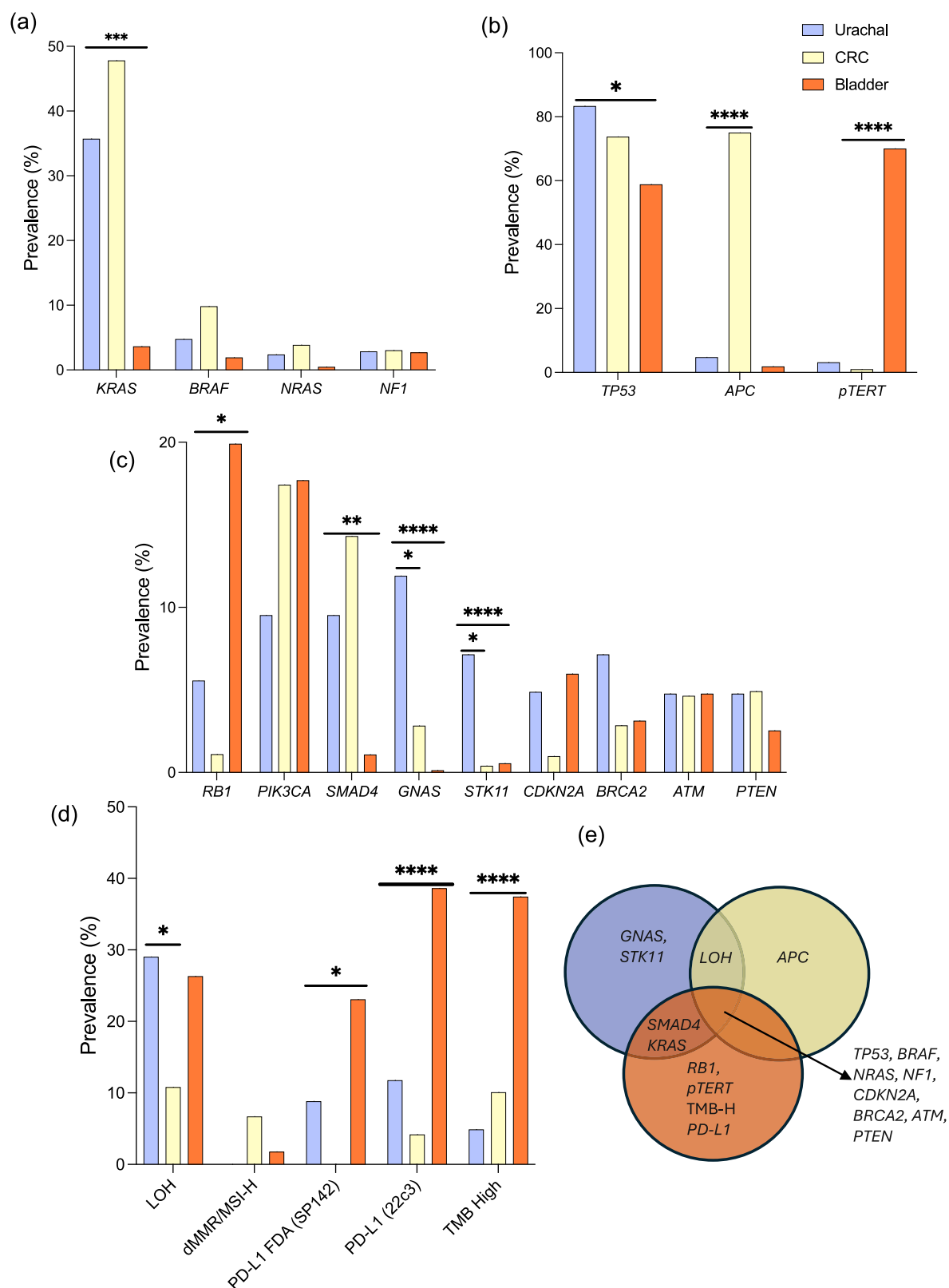


Fig. 2 | Genomic profile of urachal cancer in comparison to bladder cancer and colorectal cancer. a–c Mutational profile of urachal cancer compared to bladder and colorectal cancer. **d** Prevalence of immune-related markers and other genomic changes in urachal cancer in comparison to bladder or colorectal. **e** Venn diagram

showing unique genes with predominant mutations in urachal cancer, bladder and colorectal; genes within the intersection are relatively higher in urachal cancer compared to either bladder or colorectal. Asterisks indicates statistical significance, * $p < 0.05$, ** $p < 0.01$, *** $p < 0.001$, **** $p < 0.0001$.

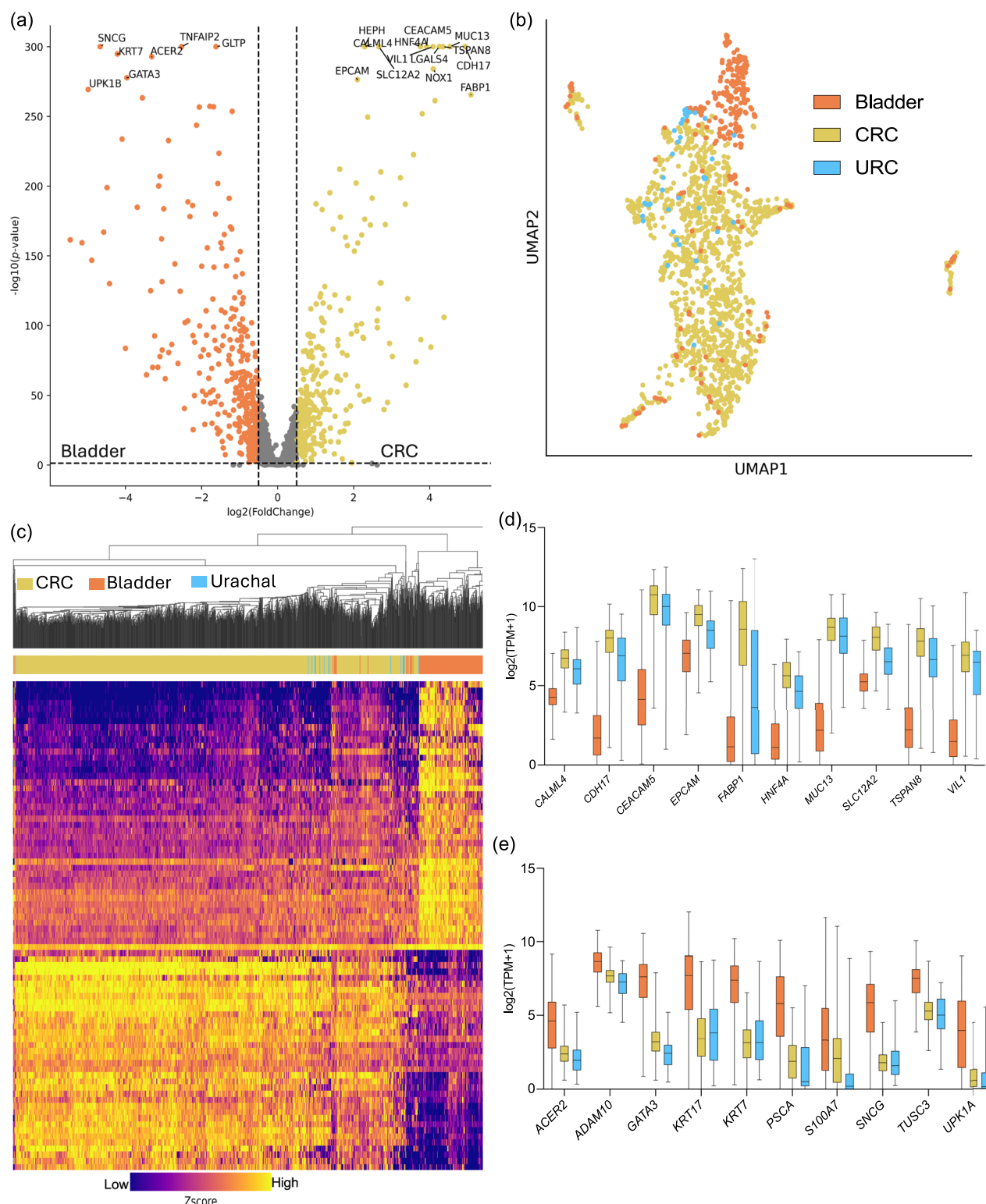


Fig. 3 | Gene expression profiling of urachal cancer in comparison to bladder and colorectal cancer. a Differentially expressed genes between bladder and colorectal cancer. **b** Uniform Manifold Approximation and Projection (UMAP) of genes expression data in urachal, bladder and colorectal cancer. **c** Comparison of top 10

highly differentially expressed genes in colorectal cancer. **d** Comparison of top 10 highly differentially expressed genes in bladder cancer. Asterisks indicates overall statistical significance, **** $p < 0.0001$.

(3.1% vs 70.0%, $p < 0.0001$) mutation, as well as decreased prevalence of PD-L1 + IHC expression (11.8% vs 38.6%, $p < 0.001$) and TMB-H (4.9% vs 37.4%, $p < 0.0001$) compared to bladder cancer – Fig. 3a–e.

To explore the similarity of urachal cancer with other tumor types, gene expression profiles were compared to those of bladder and colorectal

cancers. Firstly, differentially expressed genes were obtained between bladder cancer and colorectal cancer (Fig. 3a, d, e). Genes such as *CEACAM5*, *MUC13*, *EPCAM*, *CDH17*, and *HNF4A* were significantly observed in colorectal cancer while *GATA3*, *UPK1A*, *KRT7*, *TUSC3* and *PSCA* were significantly observed in bladder cancer. Gene expression data for colorectal,

bladder and urachal samples were projected using UMAP projection (Fig. 3b) and there was a distinct cluster and separation of most bladder cancers from colorectal, while urachal cancer samples was observed to be closely around the colorectal cancer samples. To further explore this similarity, clusters were obtained using unsupervised hierarchical clustering analysis of the top 10% differentially expressed genes between colorectal and bladder, most of the urachal cancer samples (39/41, ~95%) was observed to be clustered closely to the colorectal cancer samples – Fig. 3c. Next, differentially expressed genes were analyzed between bladder cancer and colorectal cancer. We observed that genes highly expressed in bladder cancer had lower expression in urachal cancer while those that were highly expressed in colorectal cancer were in similar order of magnitude in urachal cancer – Fig. 3d, e, Supplementary Table 1.

Furthermore, we evaluated differences in the tumor microenvironment across the three genitourinary tumors—UrC, bladder cancer, and CRC. Our findings reveal notable heterogeneity in the tumor microenvironment, with distinct immune cell fractions associated with each tumor type. Specifically, macrophage M1 cell fractions were significantly higher in CRC and UrC compared to bladder cancer, while CD8+ T cells were more abundant in CRC and bladder cancer compared to UrC. Conversely, neutrophil levels were significantly lower in UrC compared to both CRC and bladder cancer (Supplementary Table 1).

Antibody drug conjugate gene expression in urachal cancer

Given that antibody-drug conjugates (ADCs) to *HER2*, *TROP2* and *NECTIN4* are used in the treatment of bladder cancer, we compared the expression of these genes in urachal cancer to bladder and colorectal cohorts¹³. Our result (Supplementary Fig. 2) demonstrate that bladder cancer cohort had significantly higher expression levels of *HER2*, *TROP2* and *NECTIN4* compared to urachal and colorectal. The expression of these genes was comparable between urachal and colorectal cancer.

Discussion

In this study, a comprehensive characterization of the genomic landscape and tumor microenvironments of urachal cancers along with performed central pathology review was performed to examine associations with histological features that provide new insights to the biology of this rare disease. Our study found that the molecular profile of urachal cancer was similar to the findings of prior studies, with *TP53* and *KRAS* mutations being the most frequent¹². In addition, we found that more than half of urachal cancer tumors harbored alterations in the MAPK pathway, with a statistically significantly increased prevalence of *TP53* mutations in MAPK-altered tumor specimens than those without MAPK aberrations. The observation of frequent MAPK alterations in urachal cancer warrants further exploration of the use of MAPK-targeted therapy in these patients.

Further analysis, including intra-tumoral microenvironment composition and predictive markers of response to immune checkpoint inhibitors was conducted to gain better understanding of potential differences between MAPK-altered and -wild type samples. Analysis of the intra-tumoral microenvironment found low cell fractions of CD8+ T cells and monocytes in comparison to neutrophils and macrophages. Of note, the median NK cell fraction was slightly higher in MAPK-altered tumors. Further research is warranted to determine immune related biomarkers which may correlate to responsiveness to immunotherapy or cellular therapy.

Predictive markers of responsiveness to immunotherapy, such as TMB-High and PD-L1 status, were seldomly identified in urachal cancer tumors. IFN- γ has previously been shown to be associated with effectiveness of immune checkpoint inhibitors in non-small cell lung cancer and melanoma¹⁴. We found no difference in IFN- γ scores and as such, no differences in responsiveness to immunotherapy between the MAPK-altered and -wild type groups, suggesting limited IO benefit for urachal cancer patients. In our study cohort, dMMR/MSI-H, another predictive marker of IO response, was not observed in urachal cancer samples. This is somewhat different from previous studies where dMMR by IHC was observed in about 0–16.7% of urachal cancer samples^{12,15,16}.

The genomic profiles of urachal cancer, colorectal cancer, and bladder cancer had distinct alterations, with *TP53*, *GNAS* and *STK11* mutations found at a statistically higher frequency compared to colorectal cancer and bladder cancer. While loss of heterozygosity (LOH) was common between bladder cancer and urachal cancer specimens, TMB-H and PD-L1 status were more commonly found in bladder cancer samples. This finding would explain the responsiveness of immune checkpoint inhibitors in treating bladder cancer in the clinical setting and reinforces the lack of real-world data on the efficacy of immunotherapy in treating urachal cancer. Our transcriptomic analysis reinforces the observed similarity between urachal cancer and colorectal cancer as most of the urachal cancer samples distinctly clustered around colorectal samples. Moreover, given the similarity observed between urachal and colorectal cancer, future prospective interventional clinical trials for colorectal cancer may choose to incorporate urachal cancer cohorts in order to identify new therapeutics in this rare malignancy.

While this study provides a comprehensive molecular characterization of urachal cancer, along with an analysis of its immune landscape and survival outcomes, it is not without limitations. Although we observed no difference in overall survival (OS) based on MAPK status, further investigation into additional prognostic factors, such as age, sex, and disease stage, could offer valuable insights. Our analysis was also constrained by a small sample size and limited treatment data for these patients. In addition, another limitation is the retrospective nature of the study. Future studies could also explore urothelial cancers originating from urachal remnants to determine whether their molecular profiles align with those of bladder-derived urothelial cancers.

Overall, this study provides a comprehensive molecular characterization of urachal cancer and its associated immune landscape. To our knowledge, this study is the first to characterize the genomic profile of urachal cancer using DNA sequencing and RNA sequencing, while also evaluating the immune landscape of this rare malignancy. Urachal cancer tumors were rarely found to have markers of responsiveness to immune checkpoint inhibitors defined by PD-L1 and TMB high status, and thus suggestive of limited efficacy in this patient population. However, alterations in the MAPK pathway were common and as such, warrant further investigation utilizing MAPK-targeted therapies in future clinical therapeutic trials. We further revealed the broad similarity of urachal cancer to colorectal cancer, but this might require additional exploration to understand which subgroup of colorectal cancer should be considered due to the heterogeneous nature of CRC. Further understanding may provide rationale for potential inclusion of urachal cancer in prospective clinical trials evaluating investigative therapies for colorectal cancer.

Methods

Study cohort

Formalin-fixed paraffin-embedded (FFPE) samples from patients with urachal cancer ($n = 42$) were submitted to a commercial CLIA-certified laboratory for molecular profiling (Caris Life Sciences, Phoenix, AZ). The study follows the Declaration of Helsinki guidelines, Belmont Report, and U.S. Common Rule. In accordance with compliance policy 45 CFR 46.101(b), this study was conducted using retrospective, de-identified clinical data, patient consent was not required, and the study was considered Institutional Review Board exempt. All cases were centrally reviewed by a genitourinary pathologist (T.L.) to confirm histological classification. Additional cohort from bladder ($n = 6455$) and colorectal ($n = 21136$) cancer obtained from Caris Life Science database were evaluated for comparison in subset of analysis.

DNA next-generation sequencing (NGS)

In preparation of the samples for molecular testing, tumor enrichment was performed by harvesting targeted tissues using manual microdissection techniques. Genomic DNA was extracted from FFPE tissue samples and subjected to NGS using the NextSeq or NovaSeq 6000 Platforms (Illumina, Inc. San Diego, CA). A custom SureSelect XT assay (Agilent Technologies,

Santa Clara, CA) was utilized to enrich exonic regions of 592 whole-gene targets. For tumor samples sequenced on NovaSeq 6000 platform, more than 700 clinically relevant genes were assessed. All variants were detected with >99% confidence based on allele frequency and amplicon coverage, with an average sequencing depth of coverage of >500 and an analytic sensitivity threshold established of 5% for variant calling. Certified molecular geneticists examined the identified genomic variants and categorized them in alignment with the standards set by the American College of Medical Genetics and Genomics (ACMG). Calculation of mutation frequencies in individual genes included “pathogenic” and “likely pathogenic” variants, while those labeled as “benign”, “likely benign”, and “variants of unknown significance” were excluded.

Tumor mutational burden (TMB)

TMB was measured by counting all non-synonymous missense, non-sense, in-frame insertion/deletion, and frameshift mutations found per tumor that had not been previously described as germline alterations in dbSNP151, Genome Aggregation Database (gnomAD) databases, or benign variants identified by Caris’s geneticists. High TMB (TMB-H) was defined by a cut-off of ≥ 10 mutation/megabase (mut/MB) based on the KEYNOTE-158 pembrolizumab trial, where it was shown that patients with ≥ 10 mut/MB had increased response rates compared to those with < 10 mut/MB¹⁷.

Whole transcriptomic sequencing

Formalin-fixed paraffin-embedded (FFPE) tissue sections mounted on glass slides underwent staining with nuclear fast red (NFR). Regions that contained a minimum of 10% tumor content were delineated for manual microdissection and subsequent mRNA extraction. Whole transcriptome sequencing (WTS) was executed using the Illumina NovaSeq platform (Illumina, Inc., San Diego, CA) along with the Agilent SureSelect Human All Exon V7 bait panel (Agilent Technologies, Santa Clara, CA), and the resulting data reported transcripts per million (TPM).

Tumor microenvironment and gene expression profile

Immune cell fractions were inferred using the quanTIseq pipeline, a computational method for estimating immune cell fractions by deconvolution of bulk transcriptomic data¹⁸. WTS data were also used to calculate Interferon-Gamma score, as previously described¹⁹. A MAPK pathway activation score (MPAS), which serves as a transcriptomic measure of the activation state of the MAPK pathway, was calculated as the average z-score of expression values (in TPM units) for a set of 10 genes (*SPRY2*, *SPRY4*, *ETV4*, *ETV5*, *DUSP4*, *DUSP6*, *CCND1*, *PHLDA1*, *EPHA2*, and *EPHA4*), as previously described²⁰.

Global transcriptomic profiling was performed on urachal cancer using RNA sequencing data. In an attempt to better understand the relationship between urachal cancer, bladder (BLCA) and colorectal (CRC), a two-dimensional Uniform Manifold Approximation and Projection (UMAP) was utilized on integrated WTS data from these three tumor types. Furthermore, differential gene expression analysis between BLCA and CRC was performed using PyDeSeq2²¹. Clustering of CRC, BLCA and urachal cancer was performed using average linkage clustering with a centered correlation similarity metrics on the top 10% most differentially expressed genes between CRC and BLCA.

Immunohistochemistry (IHC)

IHC was conducted on complete sections of formalin-fixed paraffin-embedded (FFPE) tissues mounted on glass slides. The slides underwent staining employing automated staining methods as directed by the manufacturer. These procedures were meticulously optimized and confirmed to meet the standards outlined by CLIA/CAO and ISO. PD-L1 expression was determined using primary antibody 22c3 pharmDx (Dako, Agilent Technologies, Santa Clara, CA, USA), with a positive threshold of $\geq 10\%$ of cells stained (CPS $\geq 10\%$).

Deficient mismatch repair/microsatellite instability-high (dMMR/MSI-H)

dMMR/MSI-H was determined by a combination of immunohistochemistry (IHC) using antibodies for MLH1 (M1 antibody), MSH2 (G2191129 antibody), MSH6 (44 antibody), and PMS2 (EPR3947 antibody) from Ventana Medical Systems (Tucson, AZ), and next-generation sequencing (NGS). The outcomes from these three platforms are mostly in agreement, as previously described²². In rare instances of conflicting IHC and NGS results, the IHC results were prioritized for determining the MSI/MMR status of the tumor.

Outcome data - CODEai

Real-world overall survival (OS) information was obtained from insurance claims data and calculated from time of biopsy to last contact. Hazard ratio (HR) was calculated using the Cox proportional hazard models, and *p*-values were calculated using the log-rank test with significance determined as *p*-value of < 0.05 .

Statistics

Continuous data were assessed using a Mann–Whitney U test, and categorical data were evaluated using Chi-square or Fisher’s exact test, where appropriate. Significance was determined as *p*-value < 0.05 .

Data availability

Data is provided within the manuscript or supplementary information files.

Code availability

Not applicable.

Received: 25 September 2024; Accepted: 23 December 2024;

Published online: 11 January 2025

References

- Loizzo, D. et al. Current Management of Urachal Carcinoma: An Evidence-based Guide for Clinical Practice. *Eur. Urol. Open Sci.* **39**, 1–6 (2022).
- Benjamin, D. J. & Kalebastay, A. R. Treatment approaches for urachal cancer: Use of immunotherapy and targeted therapies. *Rare Tumors* **15**, 20363613231189984 (2023).
- Collins, D. C. et al. National Incidence, Management and Survival of Urachal Carcinoma. *Rare Tumors* **8**, 6257 (2016).
- Benjamin, D. J., Shrestha, A., Fellman, D., Cress, R. D. & Kalebastay, A. R. Association of Sociodemographic Characteristics With Survival Among Patients With Urachal Cancer in California From 1988 to 2019. *JAMA Oncol.* **8**, 1505–1507 (2022).
- Hamilou, Z. et al. Management of urachal cancer: A consensus statement by the Canadian Urological Association and Genitourinary Medical Oncologists of Canada. *Can. Urological Assoc. J.* **14**, E57–E64 (2020).
- Galsky, M. D. et al. Prospective trial of ifosfamide, paclitaxel, and cisplatin in patients with advanced non-transitional cell carcinoma of the urothelial tract. *Urology* **69**, 255–259 (2007).
- Guerin, M. et al. Urachal carcinoma: a large retrospective multicentric study from the French Genito-Urinary Tumor Group. *Front Oncol.* **13**, 1110003 (2023).
- Szarvas, T. et al. Clinical, prognostic, and therapeutic aspects of urachal carcinoma-A comprehensive review with meta-analysis of 1,010 cases. *Urol. Oncol.* **34**, 388–398 (2016).
- Kardos, J. et al. Comprehensive Molecular Characterization of Urachal Adenocarcinoma Reveals Commonalities With Colorectal Cancer, Including a Hypermutable Phenotype. *JCO Precision Oncol.* 1–12, <https://doi.org/10.1200/PO.17.00027> (2017).
- Zheng, H. & Song, W., Feng, X. & Zhao, H. Metastatic Urachal Carcinoma Treated With Several Different Combined Regimens: A Case Report. *Front. Oncol.* **11**, <https://www.frontiersin.org/articles/10.3389/fonc.2021.662589> (2021).

11. Shitara, K. et al. Phase I trial of the MET inhibitor tepotinib in Japanese patients with solid tumors. *Jpn J. Clin. Oncol.* **50**, 859–866 (2020).
 12. Reis, H. et al. Pathogenic and targetable genetic alterations in 70 urachal adenocarcinomas. *Int. J. Cancer* **143**, 1764–1773 (2018).
 13. Yu, J. et al. Novel ADCs and combination therapy in urothelial carcinoma: latest updates from the 2023 ASCO-GU Cancers Symposium. *J. Hematol. Oncol.* **16**, 85 (2023).
 14. Karachaliou, N. et al. Interferon gamma, an important marker of response to immune checkpoint blockade in non-small cell lung cancer and melanoma patients. *Ther. Adv. Med Oncol.* **10**, 1758834017749748 (2018).
 15. Zhang, X. et al. Immune Microenvironment Characteristics of Urachal Carcinoma and Its Implications for Prognosis and Immunotherapy. *Cancers* **14**, 615 (2022).
 16. Sirintrapun, S. J., Ward, M., Woo, J. & Cimic, A. High-stage urachal adenocarcinoma can be associated with microsatellite instability and KRAS mutations. *Hum. Pathol.* **45**, 327–330 (2014).
 17. Marabelle, A. et al. Association of tumour mutational burden with outcomes in patients with advanced solid tumours treated with pembrolizumab: prospective biomarker analysis of the multicohort, open-label, phase 2 KEYNOTE-158 study. *Lancet Oncol.* **21**, 1353–1365 (2020).
 18. Finotello, F. et al. Molecular and pharmacological modulators of the tumor immune contexture revealed by deconvolution of RNA-seq data. *Genome Med.* **11**, 34 (2019).
 19. Cristescu, R. et al. Pan-tumor genomic biomarkers for PD-1 checkpoint blockade-based immunotherapy. *Science* **362**, eaar3593 (2018).
 20. Wagle, M. C. et al. A transcriptional MAPK Pathway Activity Score (MPAS) is a clinically relevant biomarker in multiple cancer types. *NPJ Precis Oncol.* **2**, 7 (2018).
 21. Muzellec, B., Teleńczuk, M., Cabeli, V. & Andreux, M. PyDESeq2: a python package for bulk RNA-seq differential expression analysis. *Bioinformatics* **39**, btad547 (2023).
 22. Vanderwalde, A., Spetzler, D., Xiao, N., Gatalica, Z. & Marshall, J. Microsatellite instability status determined by next-generation sequencing and compared with PD-L1 and tumor mutational burden in 11,348 patients. *Cancer Med.* **7**, 746–756 (2018).
- Seagen. Speakers' Bureau: Merck. Travel and Accommodations: DAVA Oncology, Merck, Seagen. T.T.A. has the following disclosure: Employment: Caris Life Sciences. A.E. has the following disclosure: Employment: Caris Life Sciences. S.D. has the following disclosures: Consulting Role: BostonGene. T.L. declares no conflict of interest. R.R.M. has the following disclosures: advisory board and or consulting fees from AstraZeneca, Aveo, Bayer, Bristol-Myers Squibb, Calithera, Caris, Dendreon, Eli Lilly, Eisai, Exelixis, Janssen, Merck, Myovant, Novartis, Pfizer, Sanofi, SeaGen, Sorrento Therapeutics, Telix, and Tempus; and research support from AstraZeneca, Artera, Bayer, Bristol-Myers Squibb, Exelixis, Oncternal, and Tempus. M.J.O. has the following disclosure: Employment: Caris Life Science. A.R.K. has the following disclosures: Stock and Other Ownership Interests: ECOM Medical. Consulting or Advisory Role: AIMED BIO, Exelixis, AstraZeneca, Bayer, Pfizer, Novartis, Genentech, Bristol Myers Squibb, EMD Serono, Immunomedics, Gilead Sciences. Speakers' Bureau: Janssen, Astellas Medivation, Pfizer, Novartis, Sanofi, Genentech/Roche, Eisai, AstraZeneca, Bristol Myers Squibb, Amgen, Exelixis, EMD Serono, Merck, Seattle Genetics/Astellas, Myovant Sciences, Gilead Sciences, AVEO. Research Funding: Genentech, Exelixis, Janssen, AstraZeneca, Bayer, Bristol Myers Squibb, Eisai, MacroGenics, Astellas Pharma, BeyondSpring Pharmaceuticals, BioClin Therapeutics, Clovis Oncology, Bavarian Nordic, Seattle Genetics, Immunomedics, Epizyme. Travel, Accommodations, Expenses: Genentech, Prometheus, Astellas Medivation, Janssen, Eisai, Bayer, Pfizer, Novartis, Exelixis, AstraZeneca.

Additional information

Supplementary information The online version contains supplementary material available at <https://doi.org/10.1038/s41698-024-00795-4>.

Correspondence and requests for materials should be addressed to David J. Benjamin.

Reprints and permissions information is available at <http://www.nature.com/reprints>

Publisher's note Springer Nature remains neutral with regard to jurisdictional claims in published maps and institutional affiliations.

Open Access This article is licensed under a Creative Commons Attribution-NonCommercial-NoDerivatives 4.0 International License, which permits any non-commercial use, sharing, distribution and reproduction in any medium or format, as long as you give appropriate credit to the original author(s) and the source, provide a link to the Creative Commons licence, and indicate if you modified the licensed material. You do not have permission under this licence to share adapted material derived from this article or parts of it. The images or other third party material in this article are included in the article's Creative Commons licence, unless indicated otherwise in a credit line to the material. If material is not included in the article's Creative Commons licence and your intended use is not permitted by statutory regulation or exceeds the permitted use, you will need to obtain permission directly from the copyright holder. To view a copy of this licence, visit <http://creativecommons.org/licenses/by-nc-nd/4.0/>.

© The Author(s) 2025

Acknowledgements

None

Author contributions

Conception and Design: David J. Benjamin, Tolulope T. Adeyelu. Acquisition of Data: Tolulope T. Adeyelu, Andrew Elliott. Analysis and Interpretation of Data: David J. Benjamin, Tolulope T. Adeyelu, Andrew Elliott, Sourat Darabi, Thomas Lee, Rana McKay, Matthew J. Oberley, Arash Rezazadeh Kalebasty. Drafting of Manuscript: David J. Benjamin, Tolulope T. Adeyelu. Critical Revision of the Manuscript for Important Intellectual Content: David J. Benjamin, Tolulope T. Adeyelu, Andrew Elliott, Sourat Darabi, Thomas Lee, Rana McKay, Matthew J. Oberley, Arash Rezazadeh Kalebasty. Administrative Support: Tolulope T. Adeyelu, Andrew Elliott, Matthew J. Oberley. Supervision: Andrew Elliott, Matthew J. Oberley, Arash Rezazadeh Kalebasty.

Competing interests

D.J.B. has the following disclosures: Consulting or Advisory Role: AIMED BIO, Astellas, AVEO Oncology, Bayer, Eisai, EMD Serono, Exelixis, Janssen,